NSTX-U

Supported by U.S. DEPARTMENT OF ENERGY | Office of Science

Overview of Physics Results from the National Spherical Torus Experiment

Coll of Wm & Mary
Columbia U
CompX
General Atomics
FIU
INL
Johns Hopkins U
LANL
LLNL
Lodestar
MIT
Lehigh U
Nova Photonics
ORNL
PPPL
Princeton U
Purdue U
SNL
Think Tank, Inc.
UC Davis
UC Irvine
UCLA
UCSD
U Colorado
U Illinois
U Maryland
U Rochester
U Tennessee
U Tulsa
U Washington
U Wisconsin
X Science LLC

S. A. Sabbagh

Columbia University

for the NSTX-U Research Team

24th IAEA Energy Fusion Conference

October 9th, 2012

San Diego, California

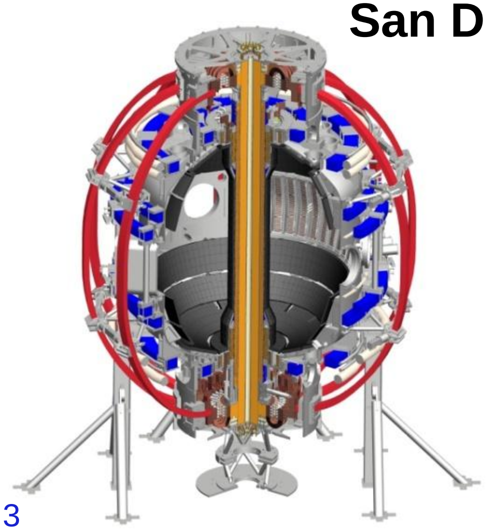

V2.3

Culham Sci Ctr
York U
Chubu U
Fukui U
Hiroshima U
Hyogo U
Kyoto U
Kyushu U
Kyushu Tokai U
NIFS
Niigata U
U Tokyo
JAEA
Inst for Nucl Res, Kiev
Ioffe Inst
TRINITI
Chonbuk Natl U
NFRI
KAIST
POSTECH
Seoul Natl U
ASIPP
CIEMAT
FOM Inst DIFFER
ENEA, Frascati
CEA, Cadarache
IPP, Jülich
IPP, Garching
ASCR, Czech Rep

NSTX research targets predictive physics understanding needed for fusion energy development facilities

- Enable devices: ST-FNSF, ST-Pilot/DEMO, ITER
  - Leveraging unique ST plasmas provides new understanding for tokamaks, challenges theory

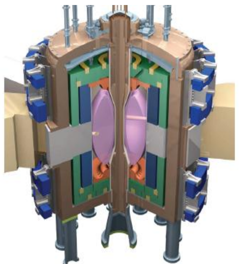

Fusion Nuclear Science Facility (FNSF)

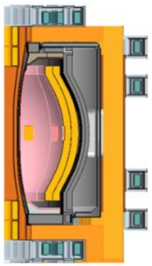

ST Pilot Plant

Outline

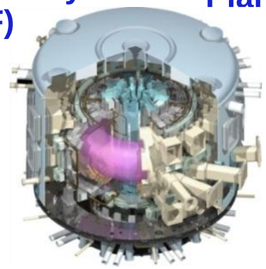

ITER

- Develop key physics understanding to be tested in unexplored, hotter ST plasmas
  - Study high beta plasma transport and stability at reduced collisionality, for extended pulse
  - Prototype methods to mitigate very high heat/particle flux
  - Move toward fully non-inductive operation

NSTX-U

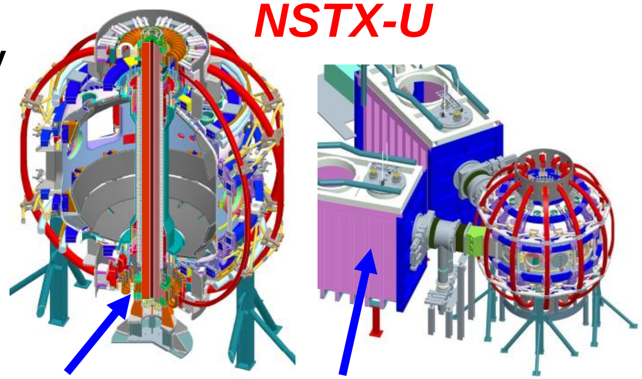

B_T	0.5 → 1 T	P_{NBI}	6 → 12 MW
I_p	1 → 2 MA	pulse	1 → 5 s

3D effects are pervasive in this research

Outline

- Transport and stability at reduced collisionality
- Pedestal transport
- High β pulse sustainment, disruptivity, and warning algorithms
- Energetic particles, power handling and first wall
- Non-inductive current and NSTX-Upgrade scenarios

τ_E scalings unified by collisionality; nonlinear microtearing simulations find reduced electron heat transport at lower ν

Experiment

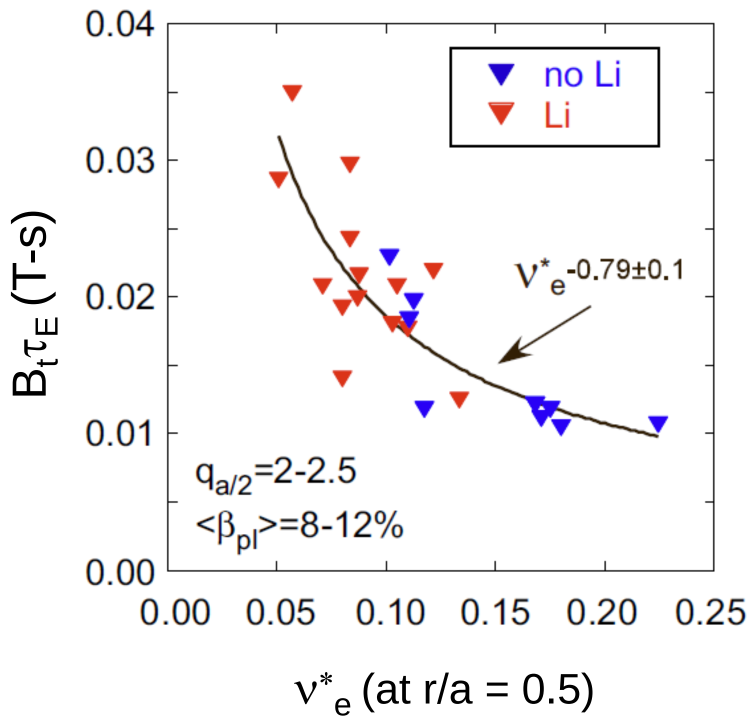

Theory

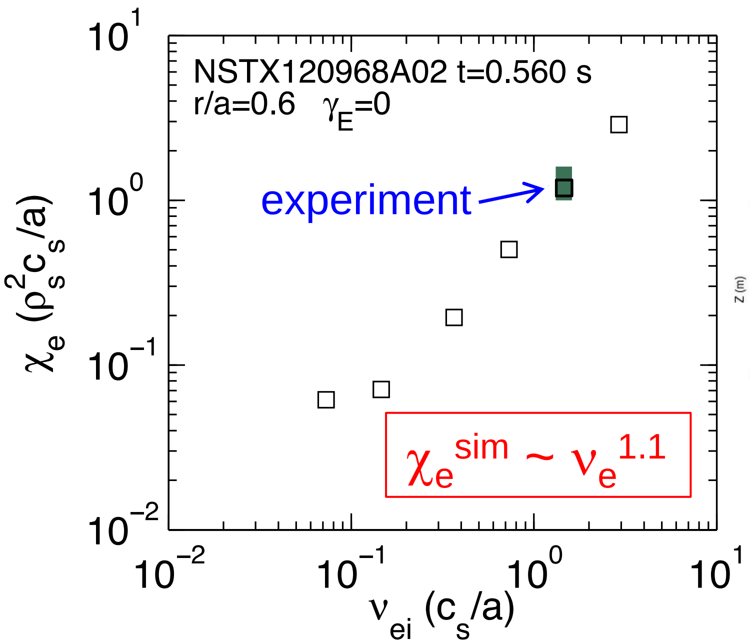

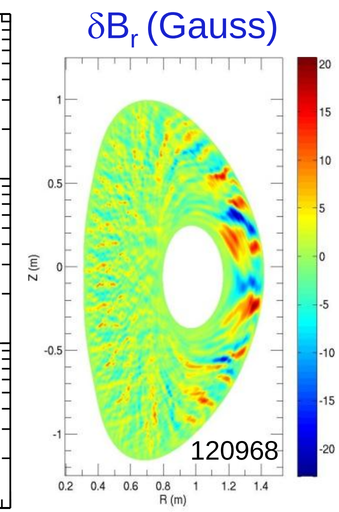

W. Guttenfelder, et al., PRL **106** (2011) 155004

- Increase in τ_E as ν^*_e decreases
- Trend continues when lithium is used

Kaye EX/7-1

- Quantitatively predicted χ_e, scaling ~ $\nu_e^{1.1}$ consistent w/experiment ($\Omega\tau_E \sim B_t\tau_E \sim \nu^*_e{}^{-0.8}$)
- Transport dominated by magnetic "flutter"
  - Significant $\delta B_r/B$ ~ 0.1%

Guttenfelder TH/6-1

- NSTX-U computed to extend studies down to < 1/4 of present ν^*

Plasma characteristics change nearly continuously with increasing lithium evaporation; reach kink/peeling limit

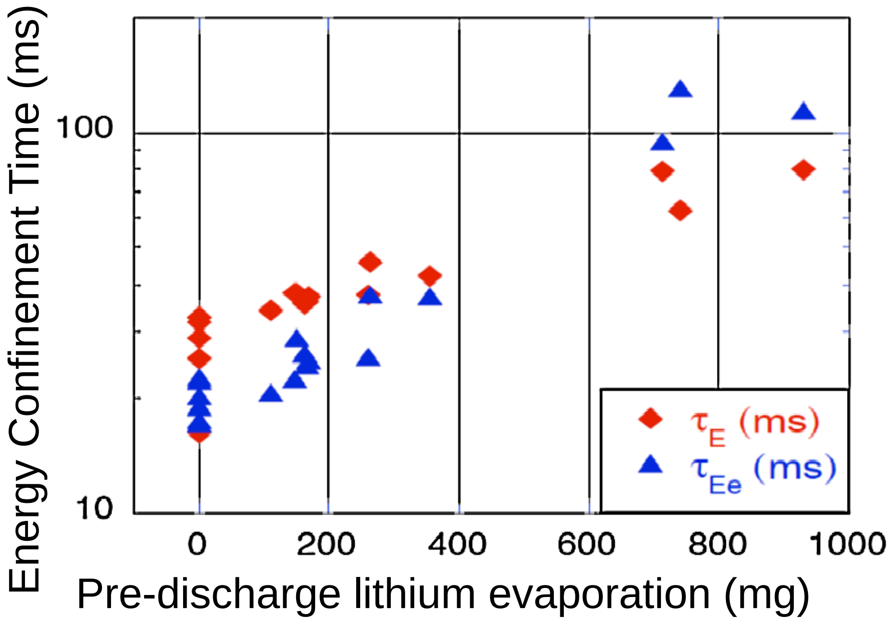

R. Maingi, et al., PRL **107** (2011) 145004

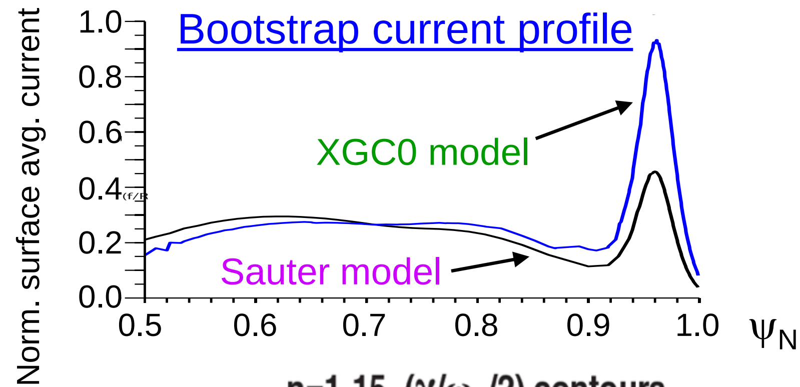

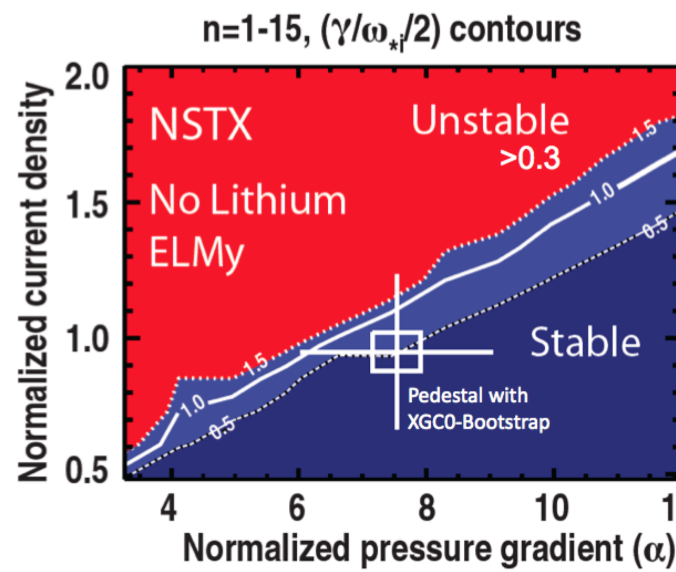

- Global parameters generally improve
  - With no core Li accumulation **Podesta EX/P3-02**
- ELM frequency declines - to zero
- Edge transport declines
  - As lithium evaporation increases, transport barrier widens, pedestal-top χ_e reduced
- New bootstrap current calculation (XGC0 code) improves agreement with profile reaching kink/peeling limit before ELM

Maingi EX/11-2 **Canik EX/P7-16** **Chang TH/P4-12** **Diallo EX/P4-04**

Simulations and lab results show importance of oxygen in the lithium-graphite PMI for pumping deuterium

- Quantum-classical atomistic simulations show surface oxygen plays key role in D retention in graphite

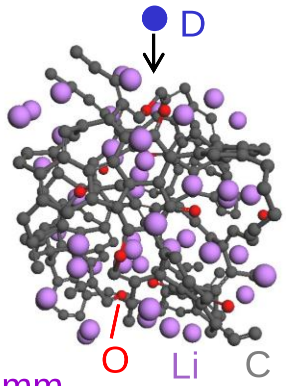

P. Krstic, sub. to Nature Comm.

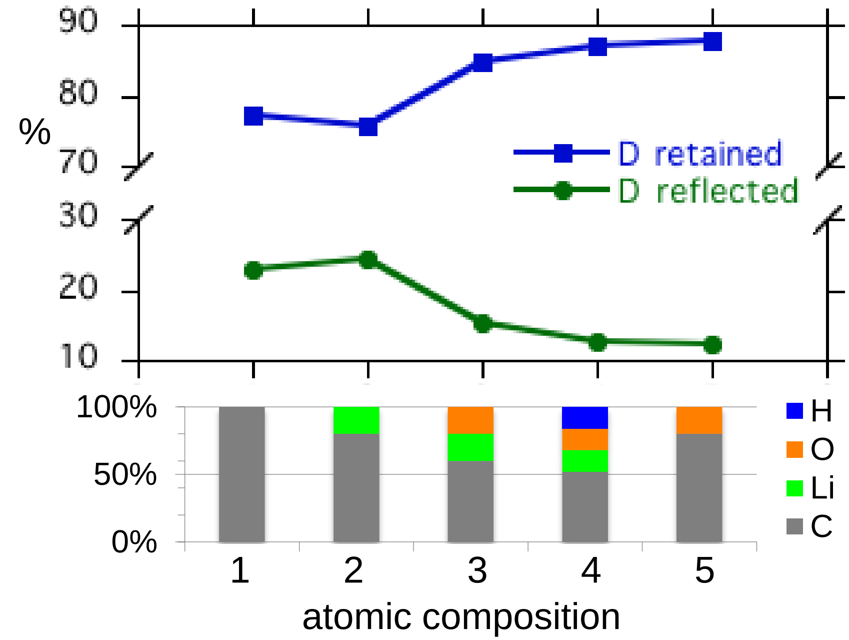

- Accordingly, lab results support that Li on graphite can pump D effectively due to O
  - Measurements show 2 μm of Li increases surface oxygen content of lithiated graphite to ~10%
  - deuterium ion irradiation of lithiated graphite greatly enhances oxygen content to 20%-40%
    - In stark contrast, D irradiation of graphite *without* Li *decreases* amount of surface O
  - Li acts as an O getter, and the O retains D

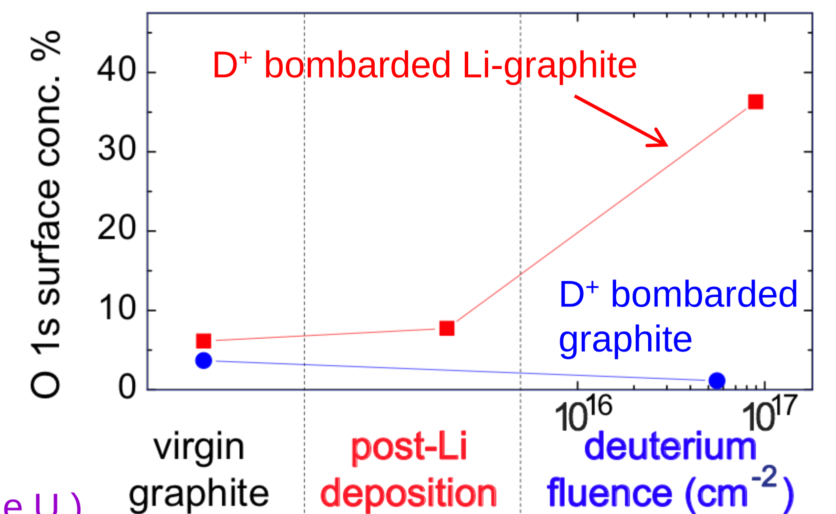

Jaworski EX/P5-31

J.P. Allain, C. Taylor (Purdue U.)

Experiments measuring global stability vs. ν further support kinetic RWM stability theory, provide guidance for NSTX-U

Theory: RWM growth rate vs. ν and ω_ϕ

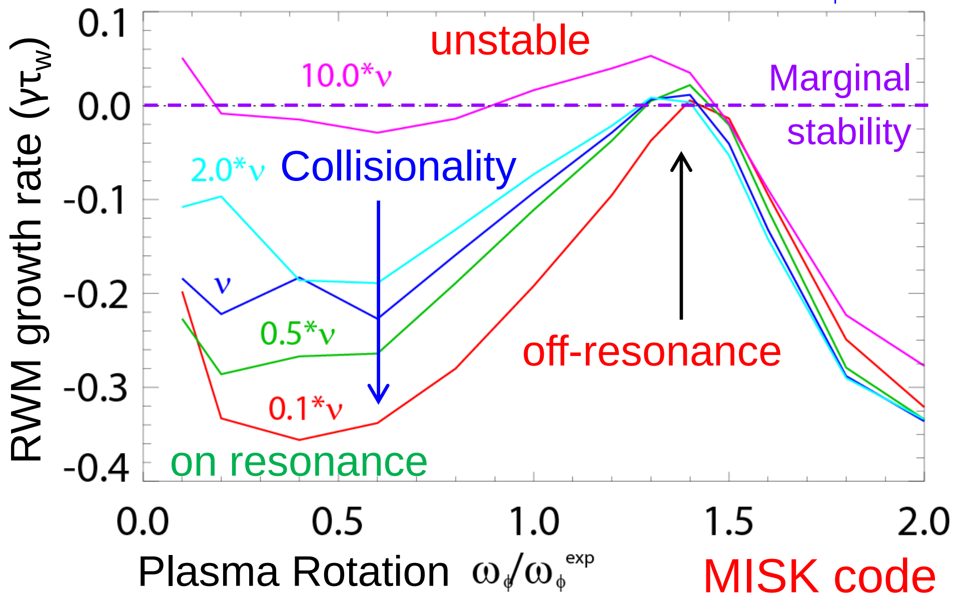

Exp: Resonant Field Amplification (RFA) vs ν

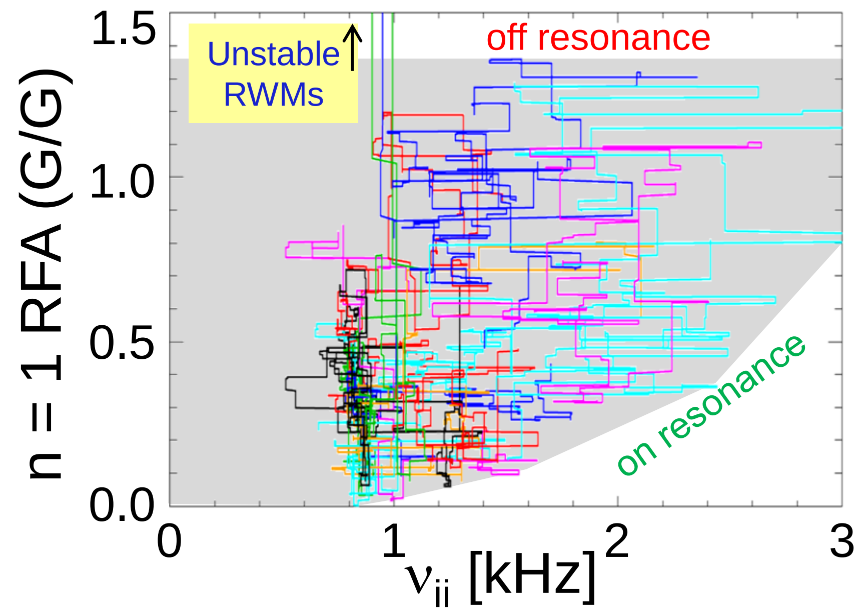

(trajectories of 20 experimental plasmas)

- Two competing effects at lower ν
  - Collisional dissipation reduced
  - Stabilizing resonant kinetic effects enhanced (contrasts early theory)
- Expectations at lower ν
  - More stabilization near ω_φ resonances; almost no effect off-resonance

J. Berkery et al., PRL **106** (2011) 075004

- Mode stability directly measured in experiment using MHD spectroscopy
  - Decreases with ν at lower RFA ("on resonance")
  - Independent of ν at higher RFA ("off resonance")

$$RFA = \frac{B_{plasma}}{B_{applied}}$$

Berkery EX/P8-07

Outline

- Transport and stability at reduced collisionality
- Pedestal transport
- High β pulse sustainment, disruptivity, and warning algorithms
- Energetic particles, power handling and first wall
- Non-inductive current and NSTX-Upgrade scenarios

BES measured low-*k* turbulence in ELM-free H-mode pedestal steep gradient region is most consistent with TEMs

Beam emission spectroscopy (BES) array

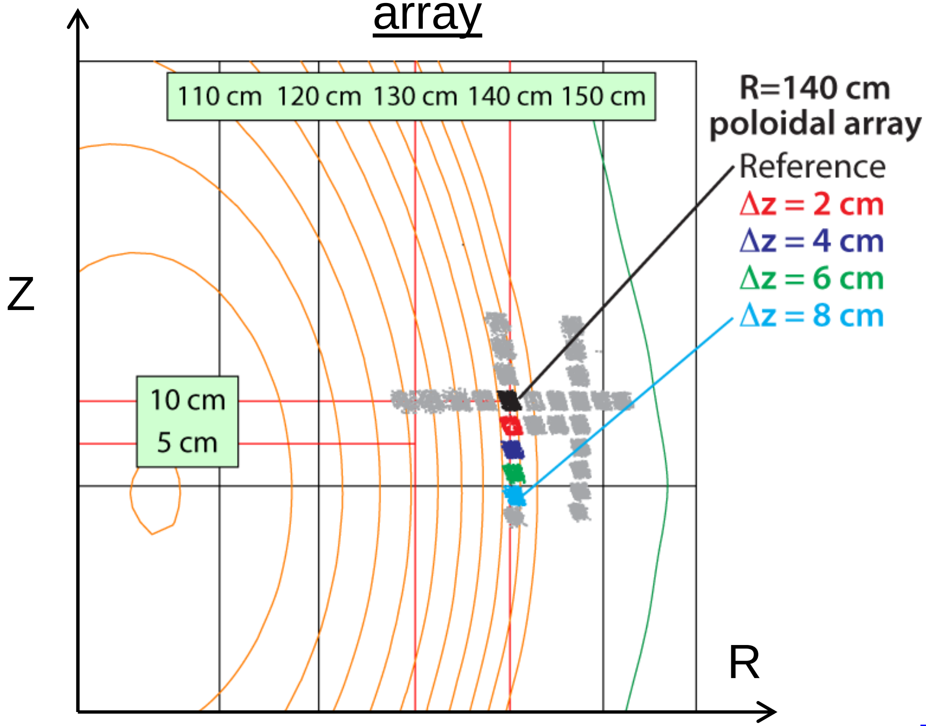

- Measurements during MHD quiet periods, in steep gradient region
- Large poloidal correlation lengths
  - $k_\theta \approx 0.2\text{-}0.4\ cm^{-1}$ and $k_\theta \rho_i \approx 0.2$

Smith EX/P7-18

Poloidal Correlation Length vs. Parameters

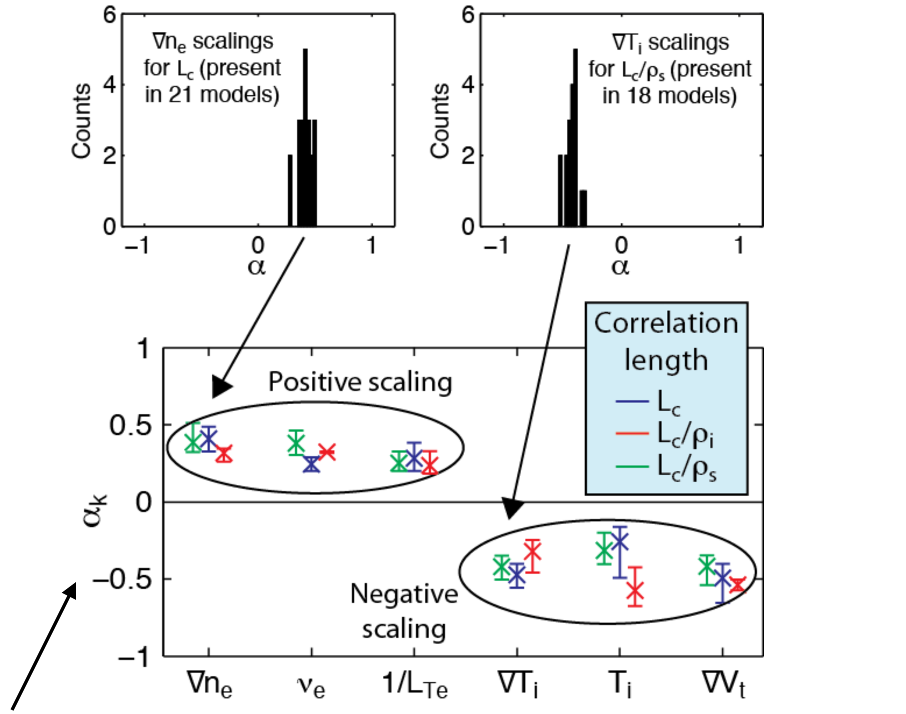

- Multivariate linear scaling coefficients α_k
- Turbulence measurements in the steep gradient of the pedestal
  - Most consistent with Trapped Electron Modes
  - Partially consistent with KBM and μ-Tearing Modes
  - Least consistent with ITG Modes

Pedestal width scaling differs from tokamaks; turbulence correlation measurements consistent with theory

Pedestal width scaling

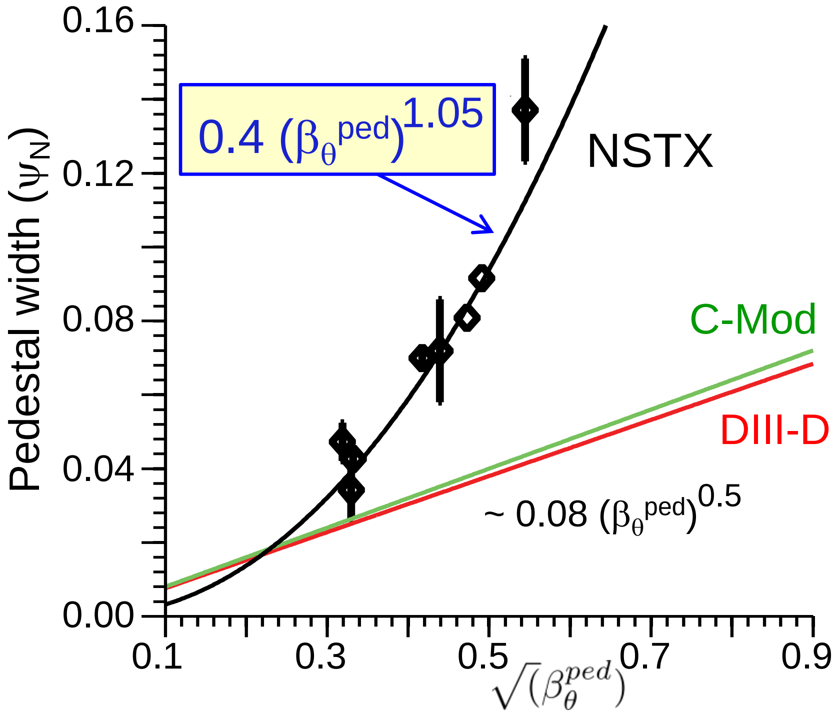

Turbulence correlation lengths

(During inter-ELM period, at pedestal top)

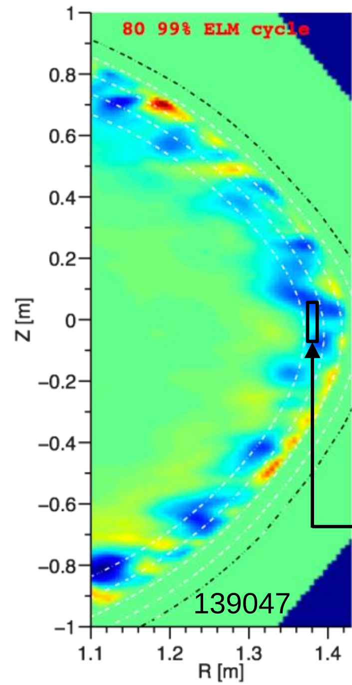

R = 1.38m

	Theory (non-linear XGC1 code)	Experiment
radial	3 cm	2 – 4 cm (reflecto-metery)
poloidal	11 cm	10 – 14 cm (BES)

80% - 99% ELM cycle

- Pedestal width scaling β_θ^α applies to multiple machines
- In NSTX, observed ped. width is larger
  - Data indicates stronger scaling: β_θ vs. $\beta_\theta^{0.5}$
  - Examining possible aspect ratio effects

- Measured correlation lengths at pedestal top are consistent with theory
  - BES and reflectometry
    - spatial structure exhibits ion-scale microturbulence ($k_\perp \rho_i$ ~ 0.2 - 0.7)
    - Compatible with ITG modes and/or KBM

Diallo EX/P4-04

A. Diallo, C.S. Chang, S. Ku (PPPL), D. Smith (UW), S. Kubota (UCLA)

Outline

- Transport and stability at reduced collisionality
- Pedestal transport
- High β pulse sustainment, disruptivity, and warning algorithms
- Energetic particles, power handling and first wall
- Non-inductive current and NSTX-Upgrade scenarios

Stability control improvements significantly reduce unstable RWMs at low l_i and high β_N; improved stability at high β_N/l_i

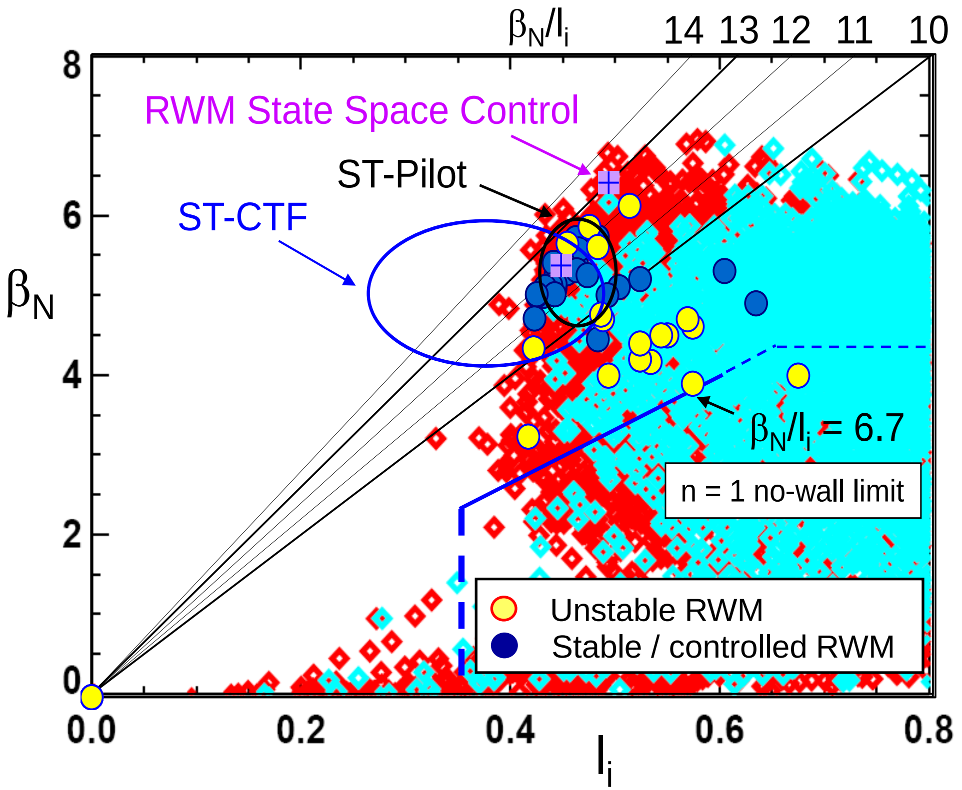

- Disruption probability reduced by a factor of 3 on controlled experiments
  - Reached 2 times computed n = 1 no-wall limit of $\beta_N/l_i = 6.7$
- Lower probability of unstable RWMs at high β_N/l_i

S.A. Sabbagh

Resonant Field Amplification (RFA) vs. β_N/l_i

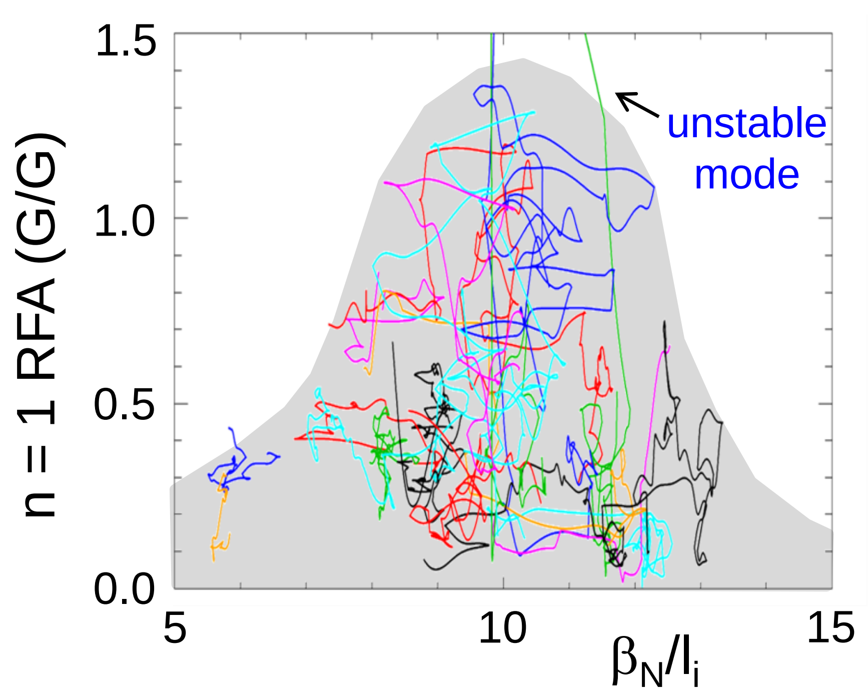

- Mode stability directly measured in experiments using MHD spectroscopy
  - Stability decreases up to $\beta_N/l_i = 10$
  - Stability increases at higher β_N/l_i
  - Presently analysis indicates consistency with kinetic resonance stabilization

Berkery EX/P8-07

Disruptivity studies and warning analysis of NSTX database are being conducted for disruption avoidance in NSTX-U

Disruptivity

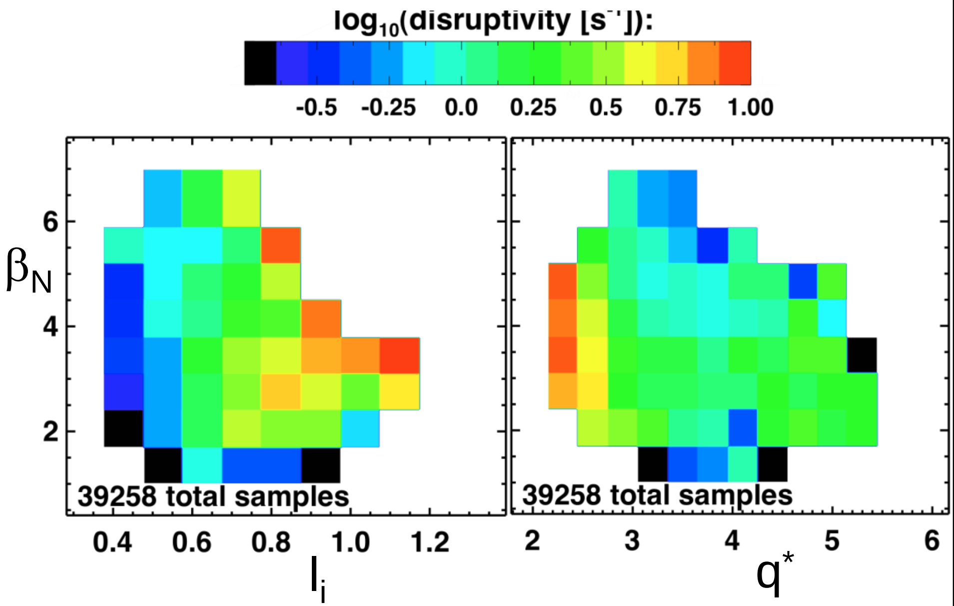

All discharges since 2006

- Physics results
  - Low disruptivity at relatively high β_N ~ 6; $\beta_N / \beta_N^{\text{no-wall}(n=1)}$ ~ 1.3-1.5
    - Consistent with specific disruption control experiments, RFA analysis
  - Strong disruptivity increase for q* < 2.5
  - Strong disruptivity increase for very low rotation

Warning Algorithms

- Disruption warning algorithm shows high probability of success
  - Based on combinations of single threshold based tests

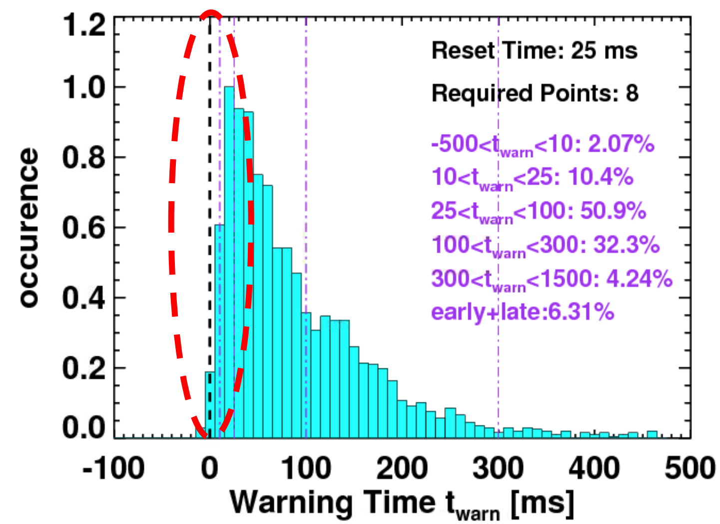

- Results
  - ~ 98% disruptions flagged with at least 10ms warning, ~ 6% false positives
  - False positive count dominated by near-disruptive events

Gerhardt EX/9-3

Improved stability control includes dual field component feedback and state space feedback, improved by 3D effects

1 Active n = 1 B_p + B_R feedback (FB) control

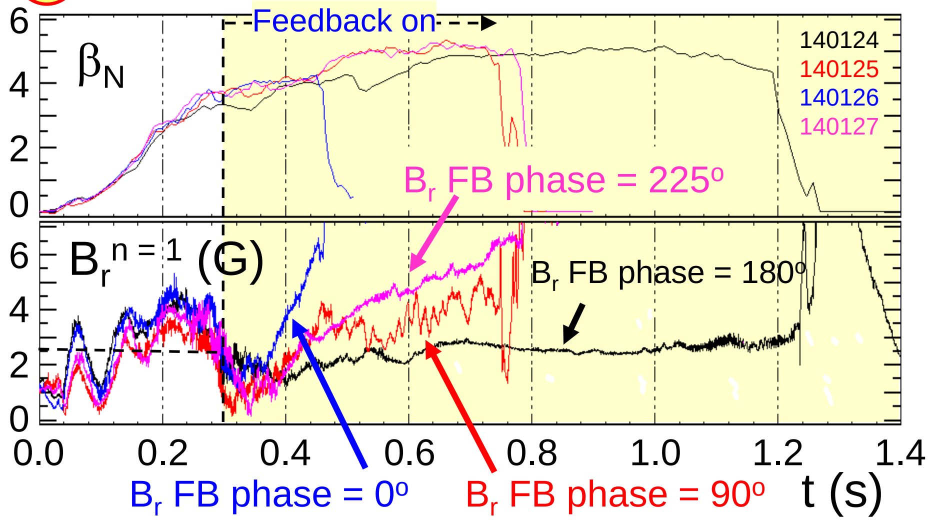

Calculation of B_r + B_p control (VALEN)

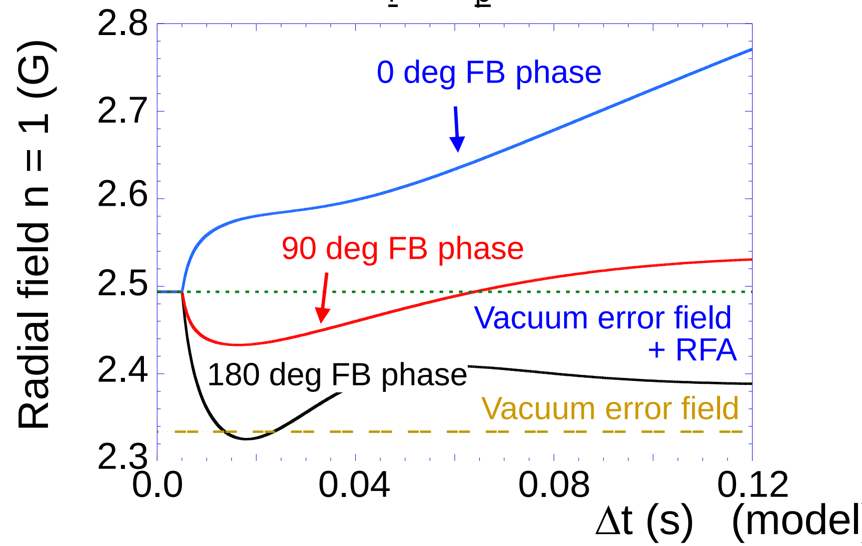

2 RWM State Space Controller

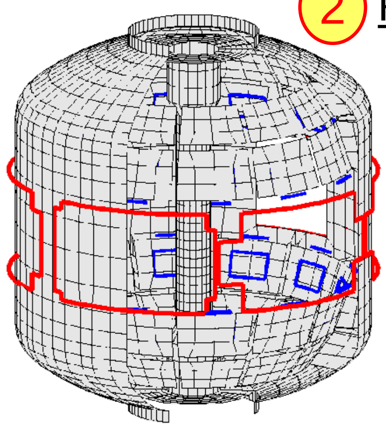

3D wall, ports, mode currents

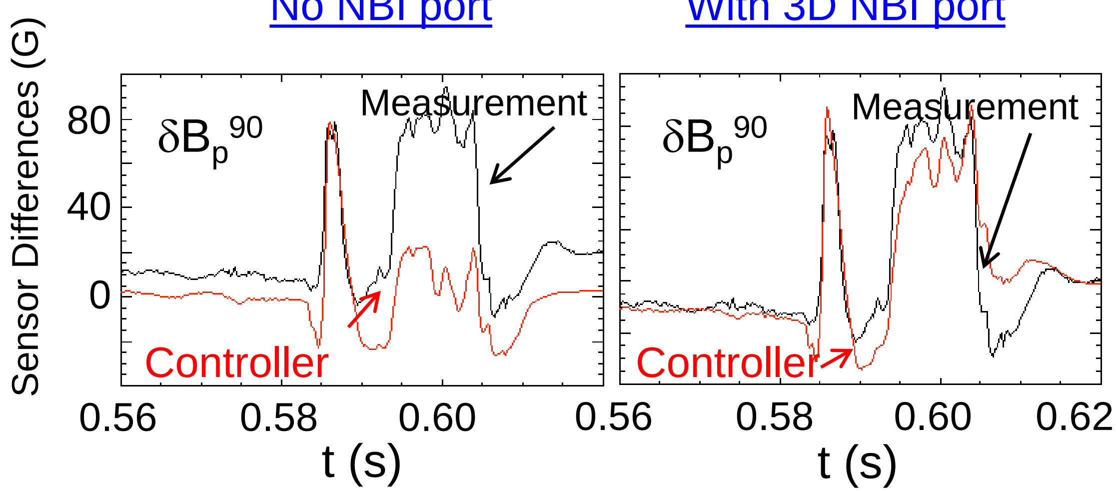

- Inclusion of 3D mode and wall detail improves control

S.A. Sabbagh, O. Katsuro-Hopkins, J.M. Bialek, S.P. Gerhardt

Outline

- Transport and stability at reduced collisionality
- Pedestal transport
- High β pulse sustainment, disruptivity, and warning algorithms
- Energetic particles, power handling and first wall
- Non-inductive current and NSTX-Upgrade scenarios

Fast ion redistribution associated with low frequency MHD measured by fast ion D_α (FIDA) diagnostic

- Caused by n = 1 global kink instabilities
- Redistribution can affect stability of *AE, RWMs, other MHD
- Full-orbit code (SPIRAL) shows redistribution in real and velocity space
  - Radial redistribution from core plasma
  - Particles shift towards $V_{||}/V = 1$
- Applied 3D fields alter GAE stability
  - By altered fast ion distribution (SPIRAL)

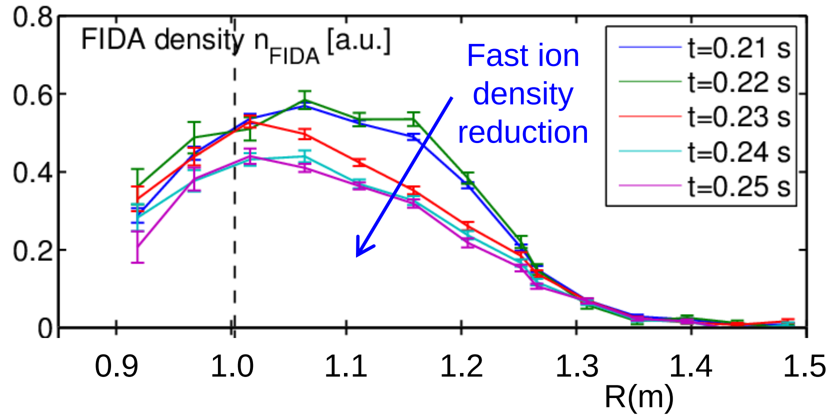

Change in distribution due to kink mode

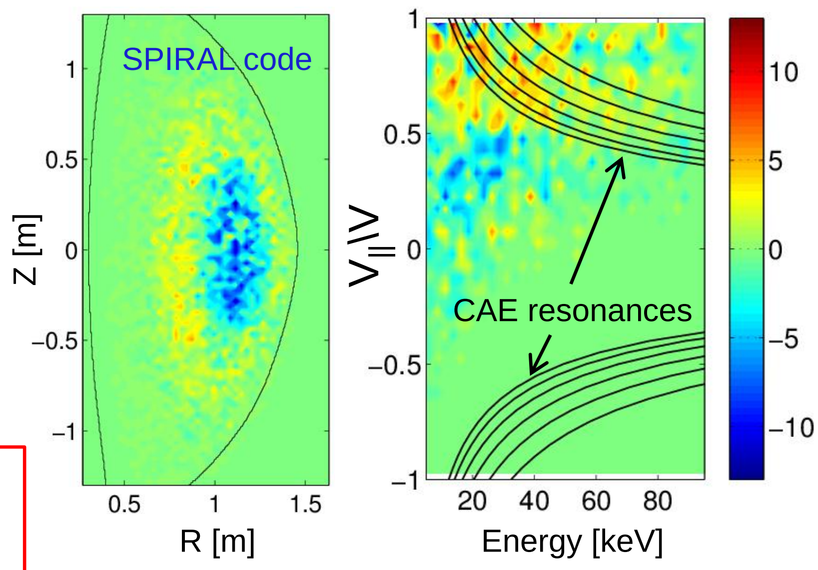

- Fast ion energy redistribution accounts for neutron rate decrease in H-mode TAE avalanches **Fredrickson EX/P6-05**
- Core localized CAE/GAEs measured in H-mode plasmas (reflectometer) **Crocker EX/P6-02**

A. Bortolon

Significant fraction of the HHFW power lost in the SOL in front of antenna flows to the divertor region

Visible camera image of edge RF power flow to divertor

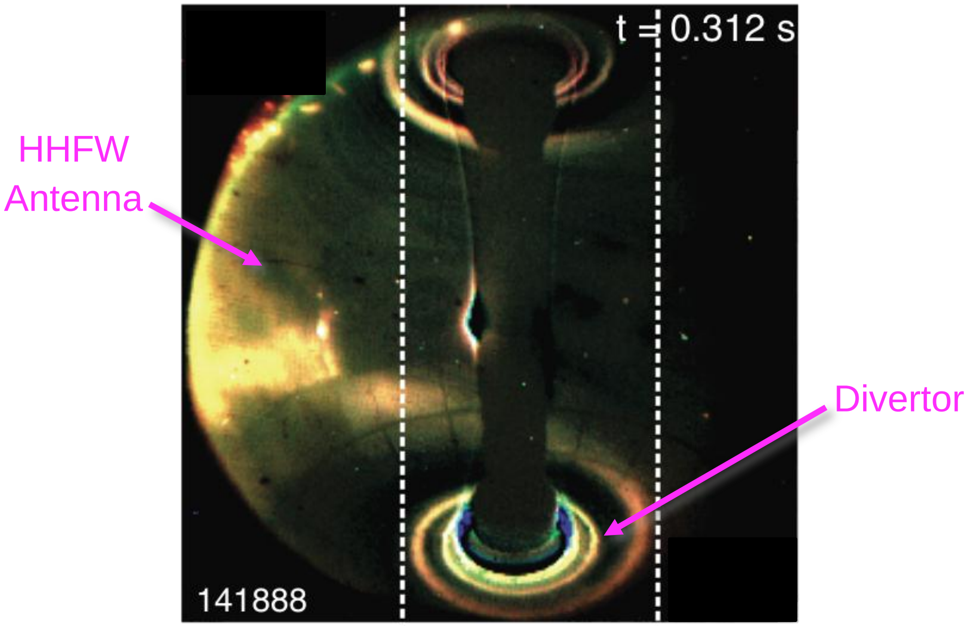

SPIRAL modeling of field lines from antenna to divertor

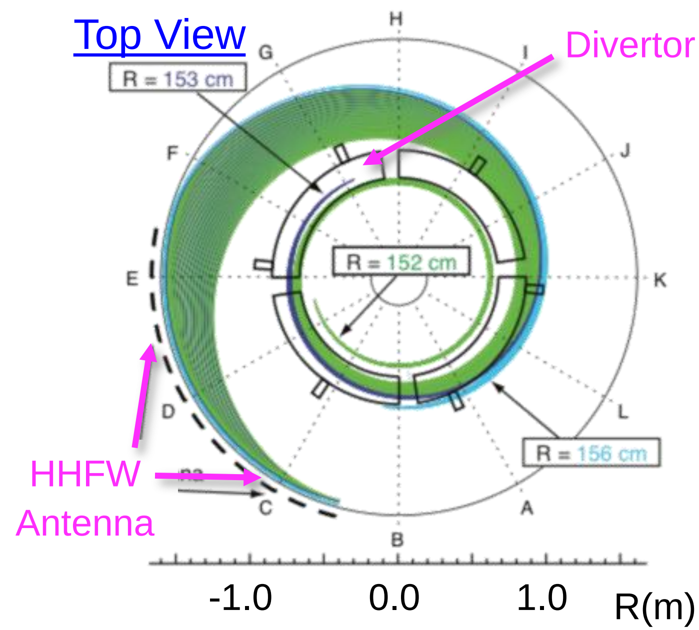

- RF power couples to field lines across entire SOL width, not just to field lines connected to antenna components
- Shows importance of quantitatively understanding RF power coupling to the SOL for prediction to future devices

R. Perkins, et al., PRL **109** (2012) 045001

Perkins EX/P5-40

Snowflake divertor experiments provide basis for required divertor heat flux mitigation in NSTX-U

- Needed, as divertor heat flux width strongly decreases as I_p increases

- Snowflake divertor experiments (P_{NBI} = 4 MW, P_{SOL} = 3 MW)
  - Good H-mode τ_E, β_N, sustained during snowflake operation
  - Divertor heat flux significantly reduced both during and between ELMs
    - during ELMs: 19 to ~ 1.5 MW/m^2
    - steady-state: 5-7 to ~ 1 MW/m^2
  - Achieved by a synergistic combination of detachment + radiative snowflake divertor

Soukhanovskii EX/P5-21

Snowflake divertor in NSTX

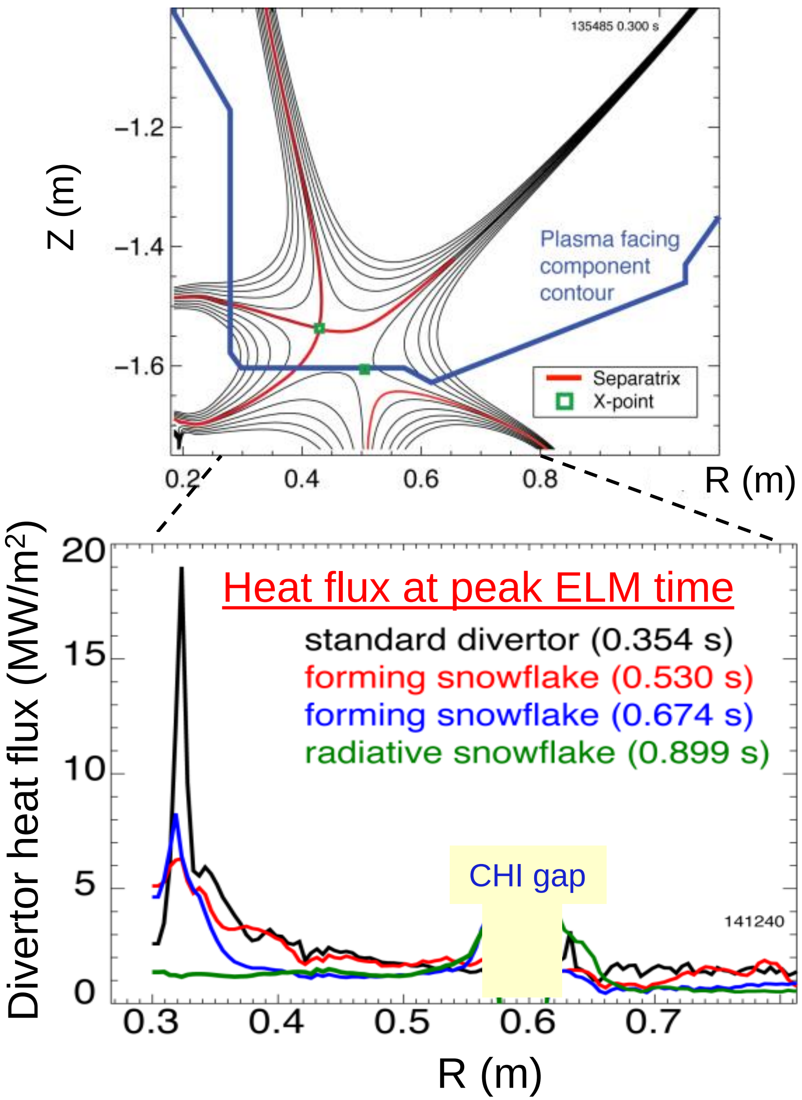

Toroidal asymmetry of heat deposition measured during standard ELMs, but decreases for 3D field-triggered ELMs

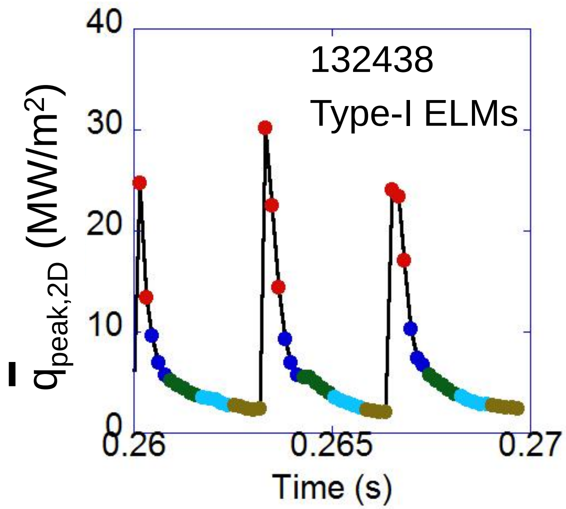

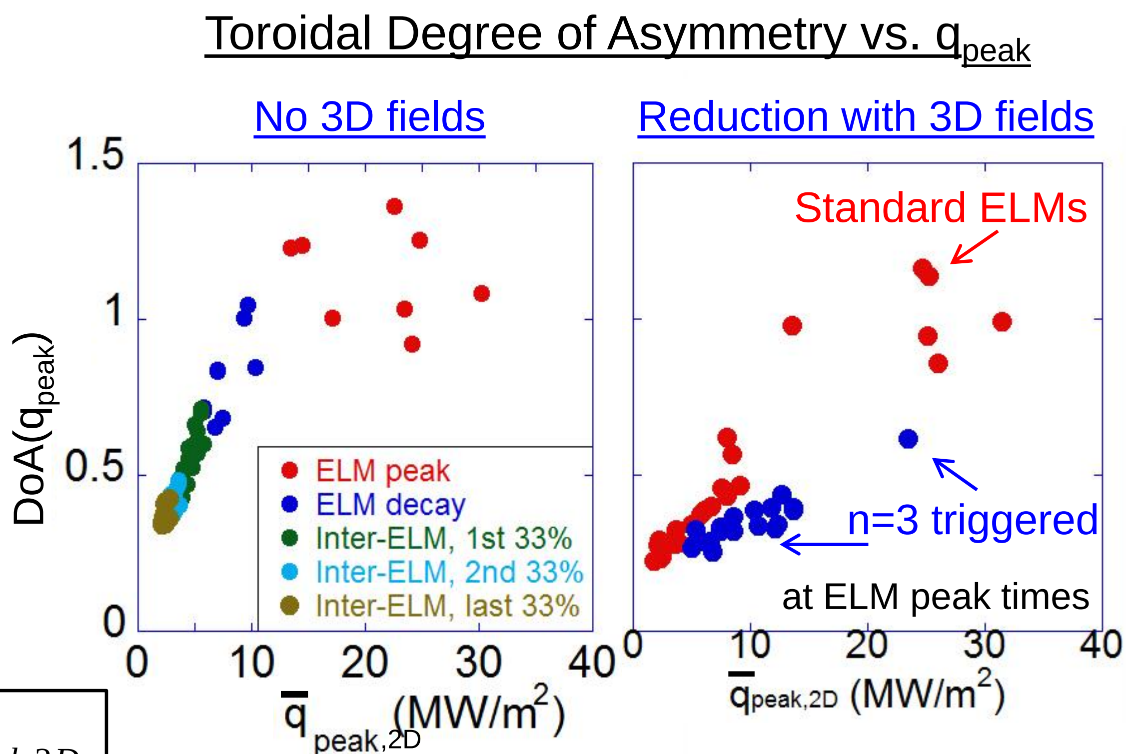

$$DoA(q_{peak}) = \sigma_{qpeak} / \bar{q}_{peak,2D}$$

- 2D fast IR camera measurement (6.3kHz), heat flux from TACO code
- Toroidal asymmetry
  - Becomes largest at the peak heat flux for usual Type-I ELMs
  - Reduced by up to 50% in ELMs triggered by n = 3 applied fields

Ahn EX/P5-33

Outline

- Transport and stability at reduced collisionality
- Pedestal transport
- High β pulse sustainment, disruptivity, and warning algorithms
- Energetic particles, power handling and first wall
- Non-inductive current and NSTX-Upgrade scenarios

Plasma discharge ramping to 1MA requires 35% less inductive flux when coaxial helicity injection (CHI) is used

CHI assisted startup in NSTX

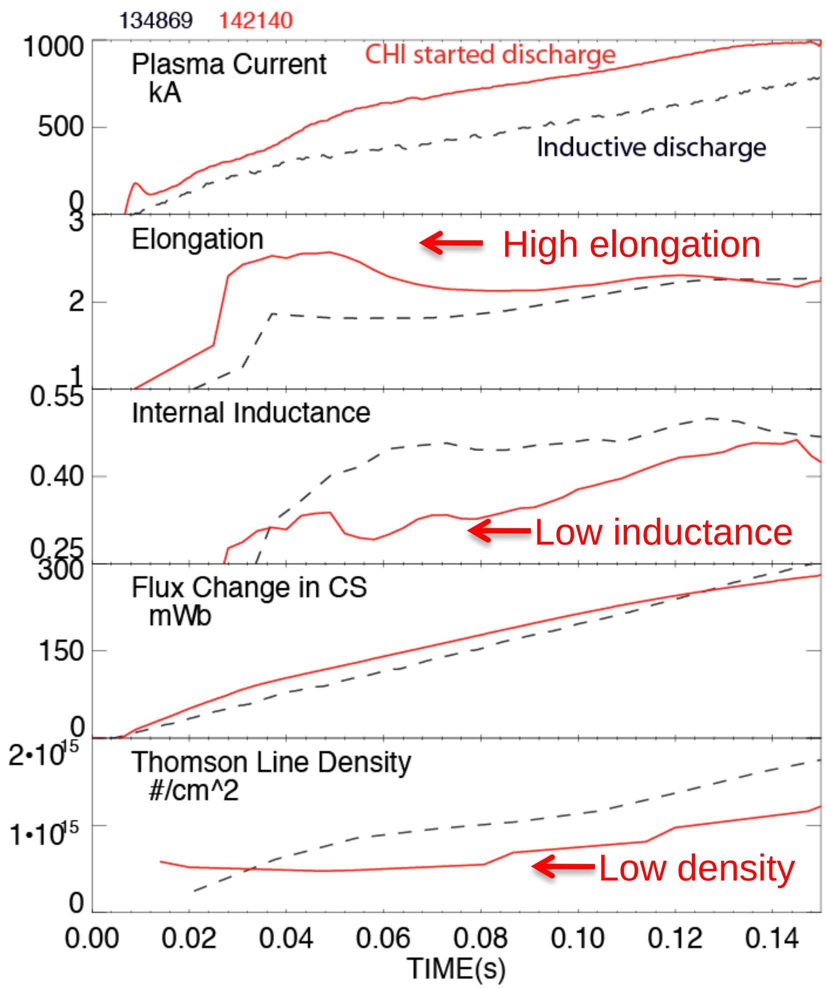

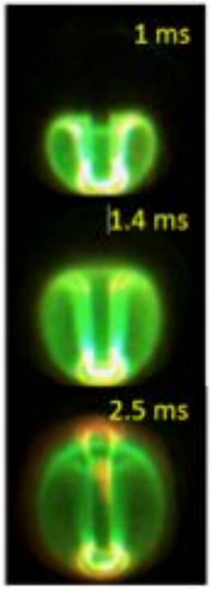

TSC simulation of CHI startup

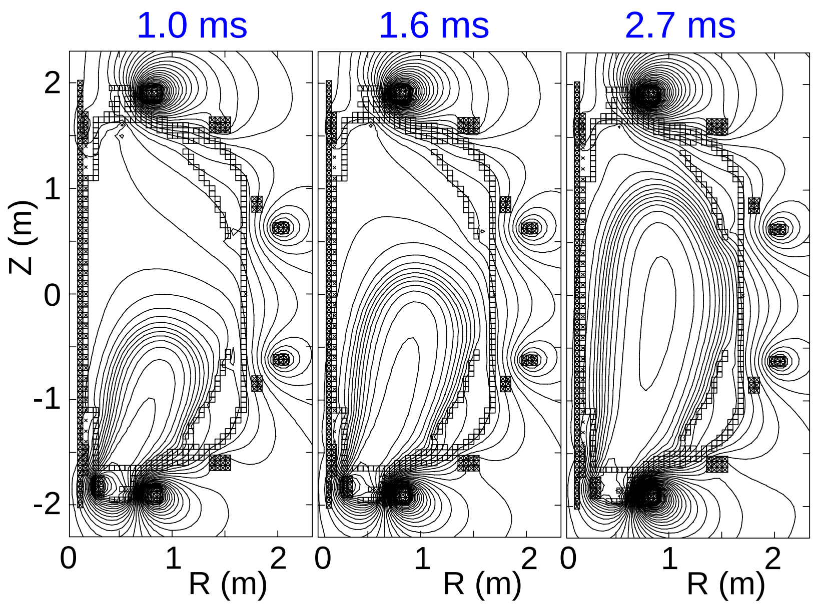

- CHI generates plasmas with high elongation, low l_i and n_e
- TSC now used for full discharge modeling to 1MA
  - CHI start-up + NBI current ramp-up
- Results imply a doubling of closed flux current > 400kA in NSTX-U

Raman EX/P2-10

Non-inductive current fractions of up to 65% sustained in NSTX, >70% transiently; Upgrade projected to achieve 100%

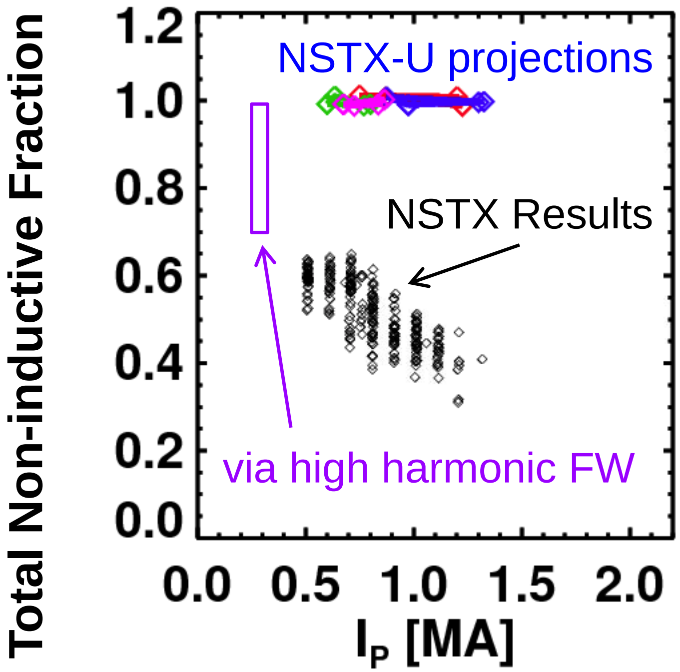

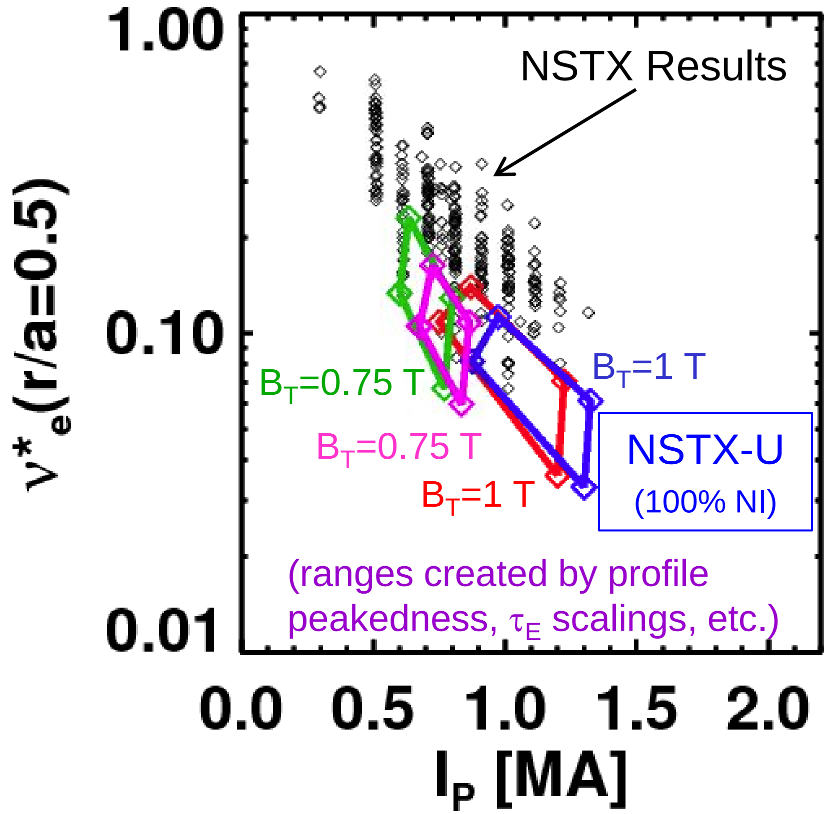

- Maximum sustained non-inductive fractions of 65% w/NBI at I_P = 0.7 MA
- 70- 100% non-inductive reached transiently using HHFW CD
  G. Taylor (Phys. Plasmas **19** (2012) 042501)

S. Gerhardt, et al., Nucl. Fusion **52** (2012) 083020

- 100% non-inductive scenarios found over wide operation range
  - Higher A ~ 1.65 of NSTX-U created in NSTX, vertical stability tested

Menard FTP/3-4 **Kolemen EX/P4-28**

Rapid Progress is Being Made on NSTX Upgrade

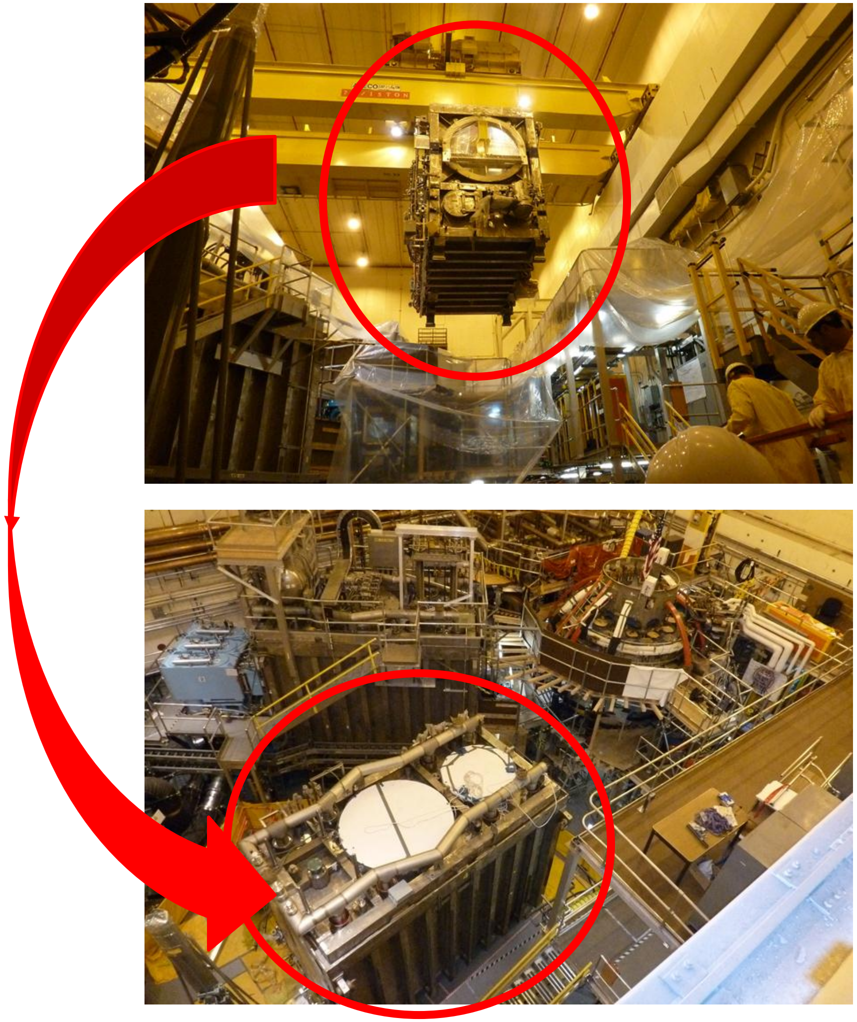

Old center stack

NEW Center Stack

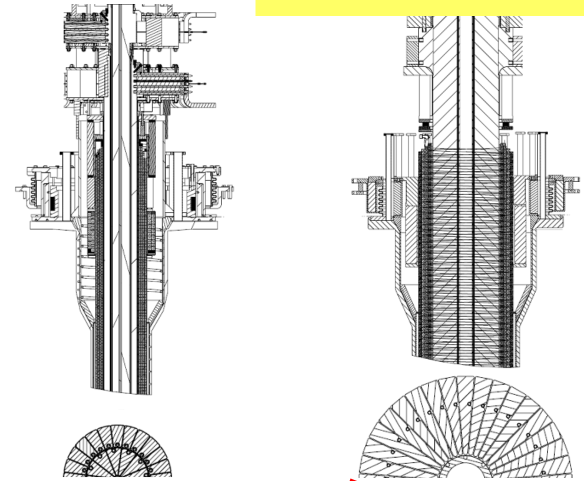

TF OD = 20cm

TF OD = 40cm

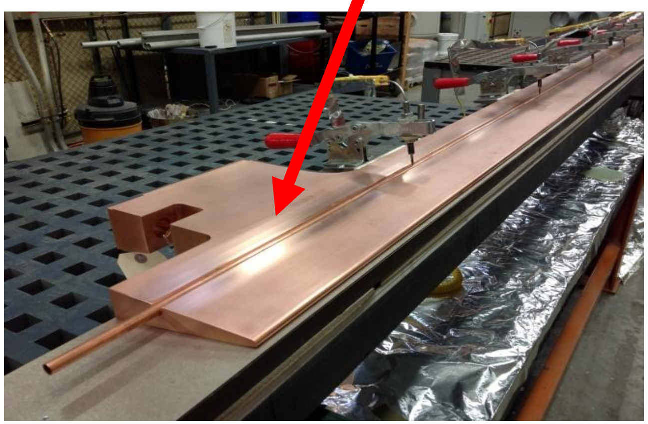

- 2nd neutral beam moved into place
- TF conductors being made

(first plasma anticipated June 2014)

Menard FTP/3-4

Continuing analysis of NSTX data targets a predictive physics understanding required for future fusion devices

- Transport and stability at reduced collisionality
  - τ_E scalings unified by collisionality; non-linear microtearing simulations match experimental χ_e, predict lower χ_e at lower ν_e* shown in experiment
  - Nearly continuous increase of favorable confinement with increased lithium
  - Stabilizing kinetic RWM effects enhanced at lower ν when near resonances
- Pedestal
  - Width scaling stronger than usual $(\beta_p^{ped})^{0.5}$; measured δn_e correlation lengths consistent w/TEMs in ped. steep gradient, non-linear gyrokinetics at ped. top
- Pulse sustainment / disruption avoidance
  - Global stability increased + low disruptivity at high β_N/l_i, advanced mode control
  - Disruption detection algorithm shows high (98%) success rate
- Power handling and first wall
  - Large heat flux reduction from combination of radiative snowflake divertor + detachment; heat asymmetry from ELMs reduced when triggered by n = 3 field
- Significant upgrade underway (NSTX-U)
  - Doubled B_T, I_p, NBI power; 5x pulse length, projected 100% non-inductive sustainment over broad operating range

NSTX Presentations at the 2012 IAEA FEC

Talks

Thursday

Progress in Simulating Turbulent Electron Thermal Transport in NSTX	**Guttenfelder**	**TH/6-1**
The Dependence of H-mode Energy Confinement and Transport on Collisionality in NSTX	**Kaye**	**EX/7-1**

Friday

Disruptions in the High Beta Spherical Torus NSTX	**Gerhardt**	**EX/9-3**
Progress on Developing the Spherical Tokamak for Fusion Applications	**Menard**	**FTP/3-4**

Saturday

The Nearly Continuous Improvement of Discharge Characteristics and Edge Stability with Increasing Lithium Coatings in NSTX	**Maingi**	**EX/11-2**

Posters

Tuesday

Lithium program	**Ono**	**FTP/P1-14**
Co-axial helicity injection	**Raman**	**EX/P2-10**
Particle code NTV simulation	**Kim**	**TH/P2-27**

Wednesday

Bootstrap current XGC	**Chang**	**TH/P4-12**
Pedestal transport	**Diallo**	**EX/P4-04**
Power scrape-off width	**Goldston**	**TH/P4-19**
Vertical stability at low A	**Kolemen**	**EX/P4-28**
Blob dynamics / edge V shear	**Myra**	**TH/P4-23**
EHOs	**Park**	**EX/P4-33**
Core lithium levels	**Podesta**	**EX/P3-02**
C, Li impurity transport	**Scotti**	**EX/P3-34**
Snowflake divertor theory	**Ryutov**	**TH/P4-18**

Thursday

Divertor heat asymmetry	**Ahn**	**EX/P5-33**
L-H power threshold vs. X pt.	**Battaglia**	**EX/P5-28**
NBI-driven GAE simulations	**Belova**	**TH/P6-16**
CAE/GAE structure	**Crocker**	**EX/P6-02**
TAE avalanches in H-mode	**Fredrickson**	**EX/P6-05**
Li deposition / power exhaust	**Gray**	**EX/P5-27**
Liquid lithium divertor results	**Jaworski**	**EX/P5-31**
RF power flow in SOL	**Perkins**	**EX/P5-40**
Snowflake divertor	**Soukhanovksii**	**EX/P5-21**

Friday

Global mode control / physics	**Berkery**	**EX/P8-07**
Edge transport with Li PFCs	**Canik**	**EX/P7-16**
Turbulence near OH L-H trans.	**Kubota**	**EX/P7-21**
ELM triggering by Li in EAST	**Mansfield**	**PD**
Electron-scale turbulence	**Ren**	**EX/P7-02**
Low-k turbulence vs. params.	**Smith**	**EX/P7-18**

Supporting slides follow

A 30% increase in L-H power threshold is found at high vs. low triangularity, consistent with X-transport theory

- X-point location is a hidden variable for L-H power threshold scaling (P_{LH})
- P_{LH} increases by 30% for high-δ vs. low-δ shape
- Consistent with predictions of X-transport theory (kinetic neo-classical transport)

Battaglia EX/P5-28

High triangularity

Low triangularity

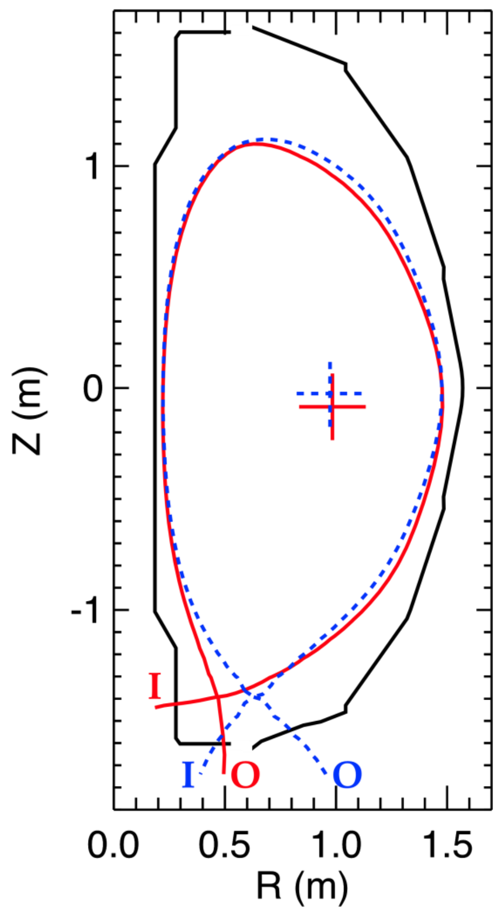

- Critical shear rate is satisfied for both shapes when core heating is 30% larger for high triangularity shape

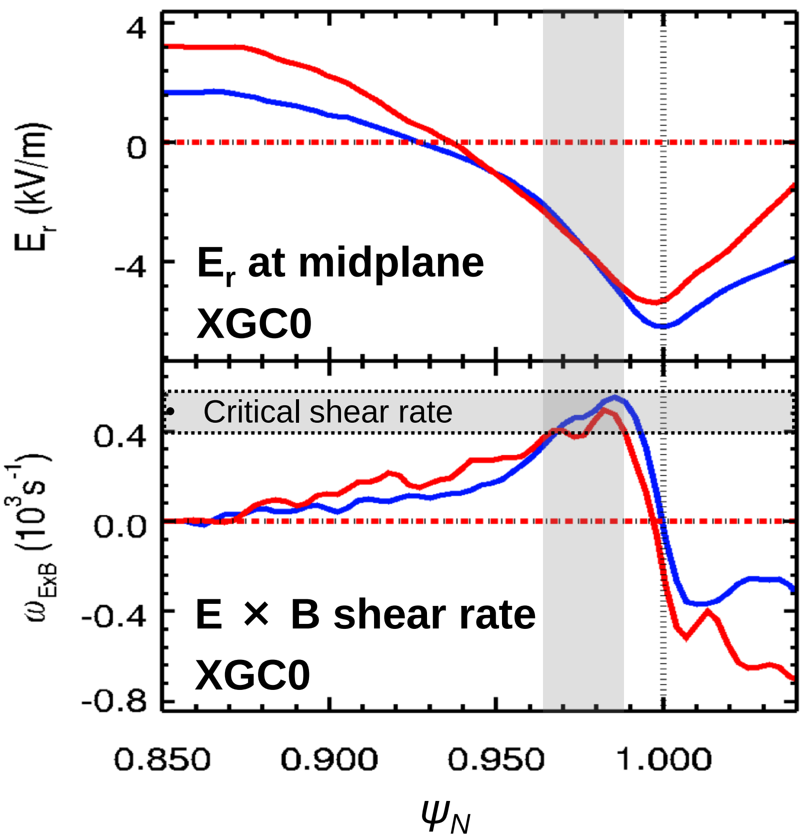

Higher aspect ratio of NSTX-U tested in NSTX, vertical stability growth rate data obtained, compared to simulation

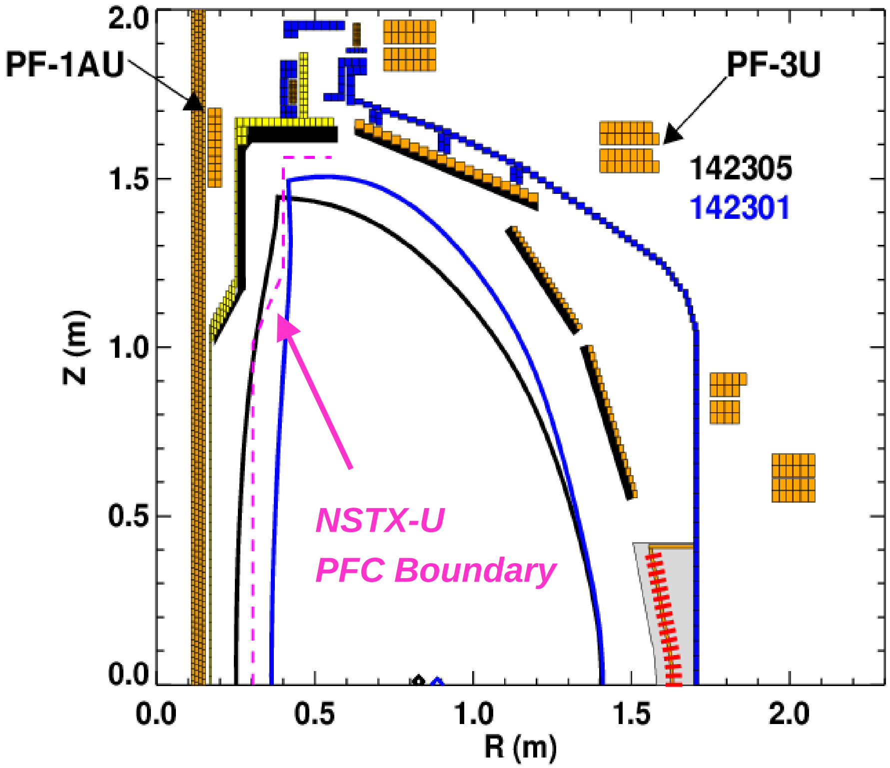

- NSTX Discharges have matched aspect ratio and elongation of NSTX-U (A = 1.65) without performance degradation

Vertical Stability Growth Rates vs. A

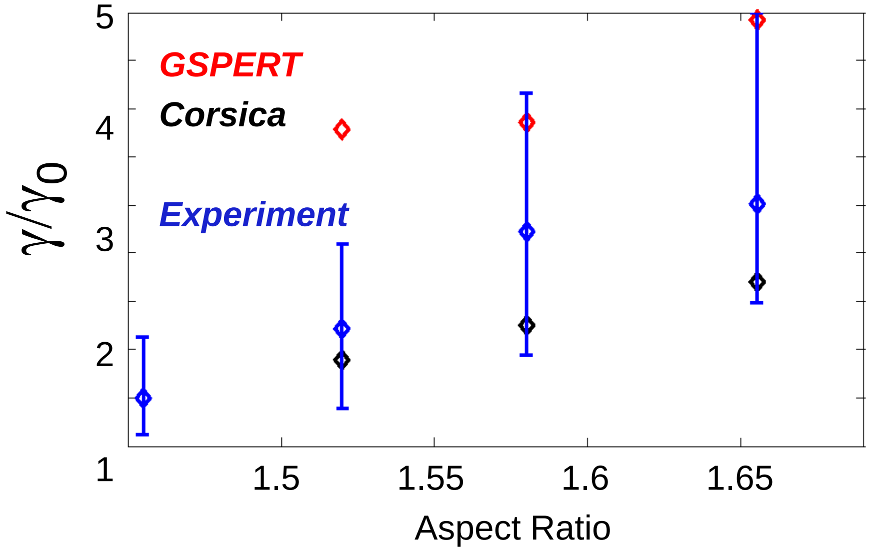

- Improvements to vertical control capability and understanding
  - Begun to compare measured growth rates to theoretical predictions (Corsica, GSPERT)
  - Improved plasma position observer
  - Modeled use of RWM coils for n=0 control

Kolemen EX/P4-28

Kinetic RWM stability theory further tested against NSTX experiments, provides guidance for NSTX-U

MISK code

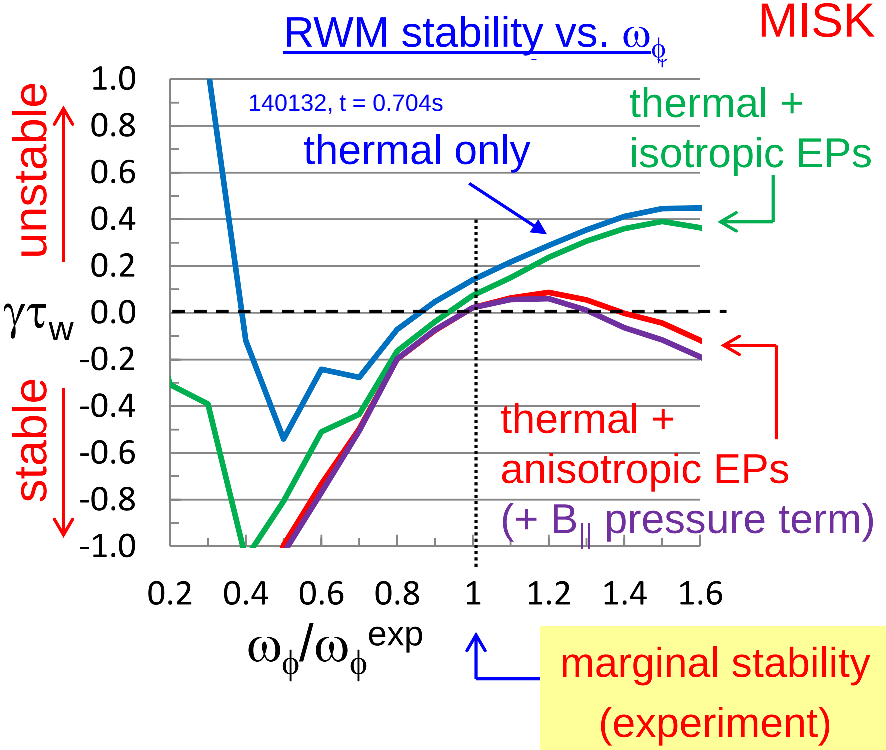

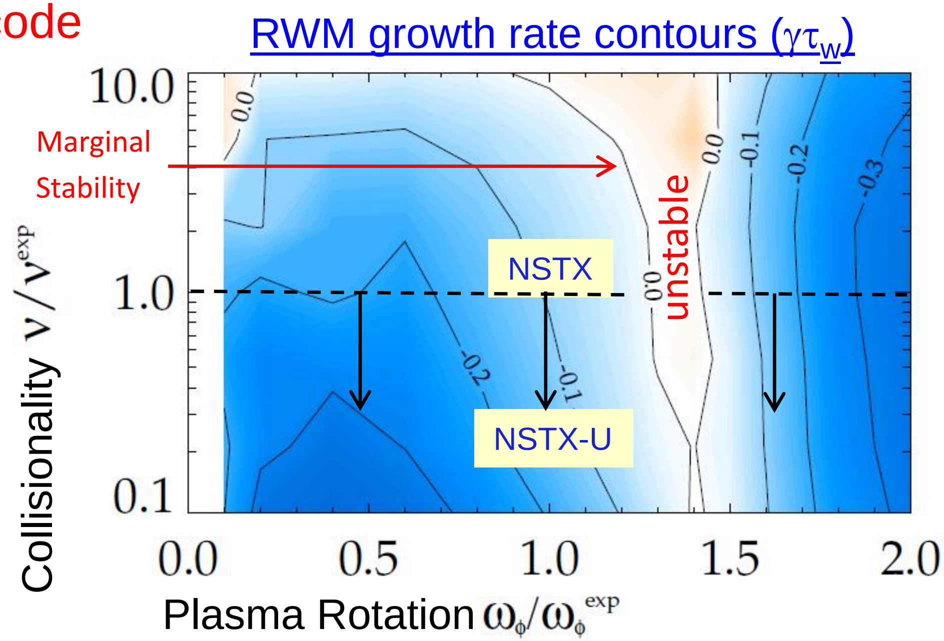

- Improvements to physics model
  - Anisotropy effects
  - Testing terms thought small
    - Already good agreement between theory and experiment of marginal stability point improved

- Two competing effects at lower ν
  - Collisional dissipation reduced
  - Stabilizing resonant kinetic effects enhanced (contrasts early theory)
- Expectations at lower ν
  - More stabilization near ω_φ resonances; almost no effect off-resonance
    - Active RWM control important

J. Berkery et al., PRL **106**, 075004 (2011)

Berkery EX/P8-07